Thin Solid Films 519 (2011) 3283–3287

Contents lists available at ScienceDirect

Thin Solid Films

journal homepage: www.elsevier.com/locate/tsf

# Optical properties of thermochromic $VO_2$ thin films on stainless steel: Experimental and theoretical studies

A. Lafort [a,*], H. Kebaili [b], S. Goumri-Said [c], O. Deparis [c], R. Cloots [a], J. De Coninck [b], M. Voué [b,d], F. Mirabella [e], F. Maseri [e], S. Lucas [c]

[a] Université de Liège, ULg, GreenMAT-LCIS, 3 Allée de la chimie, bat B6a, 4000 Liège, Belgium
[b] Université de Mons, UMONS, Laboratoire de physique des surfaces et interfaces, 20 Place du Parc, 7000 Mons, Belgium
[c] University of Namur (FUNDP), Research Centre in Physics of Matter and Radiation (PMR), 61 Rue de Bruxelles, 5000 Namur, Belgium
[d] Université de Mons, UMONS, Physique des matériaux et optique, 20 Place du Parc, 7000 Mons, Belgium
[e] ArcelorMittal Liège Research, Boulevard de Colonster B57, 4000 Liège, Belgium

ARTICLE INFO

*Article history:*
Received 27 May 2010
Received in revised form 9 December 2010
Accepted 10 December 2010

*Keywords:*
Vanadium oxide
Thermochromic materials
Thin films
Multi-layer optical model
Reflectance spectra
Spectroscopic ellipsometry

ABSTRACT

Thermochromic films of $VO_2$ were deposited by DC reactive magnetron sputtering on stainless steel substrate. Complex refractive indexes of $VO_2$ were determined by ellipsometric spectroscopy (0.35–16.5 μm) for different film thicknesses. Optical simulations were performed to model the spectral reflectance of the film/substrate system for a film thickness of 100 nm and 200 nm and to monitor the optical contrast of the thermochromic layers by comparing the spectral reflectance at 25 °C and 100 °C. The good agreement observed between experimental and theoretical spectra demonstrates the adequacy of the model for predicting the optical properties of the samples.



## 1. Introduction

Under temperature change, vanadium dioxide undergoes an abrupt reversible phase transition from a semiconducting phase to a metallic phase. This transition, due to a monoclinic to tetragonal structural transition, is accompanied by a spectacular modification of the optical properties. Below 68 °C, the monoclinic semiconducting phase material transmits infrared radiation while above 68 °C the tetragonal metallic phase material becomes reflective. This thermochromic behaviour has motivated the study of vanadium dioxide as a coating material. Up to now, $VO_2$ thin films have been deposited on transparent substrates as smart coatings for passive solar heat control [1–6].

Preparation of thermochromic $VO_2$ by reactive magnetron sputtering is quite sensitive to process parameters. To obtain useful thermochromic $VO_2$ films, two conditions are required: a high crystallinity and the exact stoechiometry. Due to the complexity of the V–O phase diagram, the synthesis of a single phase of vanadium dioxide requires the accurate control of critical parameters such as substrate temperature and oxygen partial pressure in the deposition chamber [7].

In this paper, we report the growth of thermochromic $VO_2$ thin films on stainless steel substrate by reactive DC magnetron sputtering. Chemical composition and structural properties as functions of the oxygen flux are reported as well as the film optical properties of thermochromic films. Complex refractive indexes of deposited layers have been extracted from spectroscopic ellipsometry measurements and used to establish a realistic optical model in order to predict and to optimise the optical contrast between both thermochromic states. Ellipsometric measurements have been previously reported for thin films prepared by magnetron sputtering but in a narrower wavelength range than in our work [4,8–11].

## 2. Experimental methods

Thin films of $VO_2$ ($5 \times 5$ cm$^2$) were deposited on stainless steel (SS) substrate in a reactive DC magnetron sputtering system (AJA international). The dimensional and process parameters are listed in Table 1. The reactive gas was introduced in the chamber through a ring near the substrate. The working pressure in the chamber was regulated during the deposition by an adaptive pressure controller valve, and the flow was kept constant for every $Ar/O_2$ gas flow.

* Corresponding author.
*E-mail address:* adeline.lafort@arcelormittal.com (A. Lafort).

0040-6090/$ – see front matter © 2010 Elsevier B.V. All rights reserved.
doi:10.1016/j.tsf.2010.12.122

**Table 1**
Sputtering parameters of $VO_x$ thin films.

| | |
|---|---|
| Vacuum | $1.3\times10^{-8}$ Pa |
| Total pressure | $1.3\times10^{-4}$ Pa |
| Target | ∅ 2 in., V (99.98%) |
| DC power | 200 W |
| Ar flow rate | 20 sccm |
| $O_2$ flow rate | 1–7 sccm |
| Substrate temperature | 480 °C |
| Distance target—substrate | 15 cm |
| Thickness | 100–300 nm |

Films were firstly characterized by grazing incidence X-ray diffraction (Bruckers D8, CuKα radiation 40 kV, 40 mA). The film microstructure was studied by scanning electron microscopy at 3 kV (FEG-Zeiss ultra 55). A cross section polisher (JEOL SM-09010) was used to prepare cross sections of the samples. Film thicknesses were evaluated by profilometry (Veeco Dektak 6 M) on a step prepared by masking a part of the heated substrate during the $VO_2$ film formation. Total reflectance spectra in the wavelength range of 0.25–15 μm were measured by using a Lambda 950 UV-VIS-NIR spectrophotometer (Perkin Elmer) and Nexus FTIR spectrophotometer (Thermo VG). In order to monitor the optical properties versus temperature, samples were heated within a Linkam cell (PE 100 heating cell and PE94 controller) with an accuracy of 0.1 °C. The optical transition was studied by recording the NIR reflectance at 2.5 μm at different temperatures.

The ellipsometric measurements were carried out with a Sopra GESP5 rotating polarizer instrument operating in the visible and near-infrared spectral ranges. The ellipsometric angles Ψ and Δ were measured in the range 0.35–1.65 μm with a spectral resolution of 0.01 μm. The polarizer was rotated at 9 Hz. Measurements were carried out at 70° of incidence in a parallel beam configuration (lateral resolution: 4 mm). In the mid-infrared spectral domain, a GES-FTIR ellipsometer (Sopralab, France) was used. In this case, the wavelength range covered by the instrument was 1.65–16.5 μm and the spectral resolution was 0.05 μm. The temperature of the sample was controlled using a Linkam heating/cooling stage with a precision of 0.1 °C. The ellipsometric data were processed using the Winelli software (Sopralab, France).

## 3. Theoretical modelling of optical properties

Theoretical reflectance spectra were calculated using the continued-fraction method, which relies on exactly solving Maxwell's equations for an arbitrarily stratified medium [12]. In this method, the reflection coefficients for transverse-electric or transverse-magnetic polarized light are expressed in terms of the surface impedances, which take the form of continued fractions. These continued fractions terminate for a finite number of layers deposited onto an infinitely thick substrate (of known refractive index). Their values are determined as soon as the thickness and the refractive index of all the layers are known and the incidence conditions are given. The reflectance is calculated from the value of the surface impedance at $z=0$, i.e. at the interface between the incidence medium and the first layer of the stack. Complex refractive index data which were obtained from ellipsometric spectral measurements were used as inputs in the calculation programme.

## 4. Results and discussion

### 4.1. Film deposition

In the oxygen reactive sputtering of vanadium, the discharge voltage and the deposition rate depend on the oxygen flux (Fig. 1).

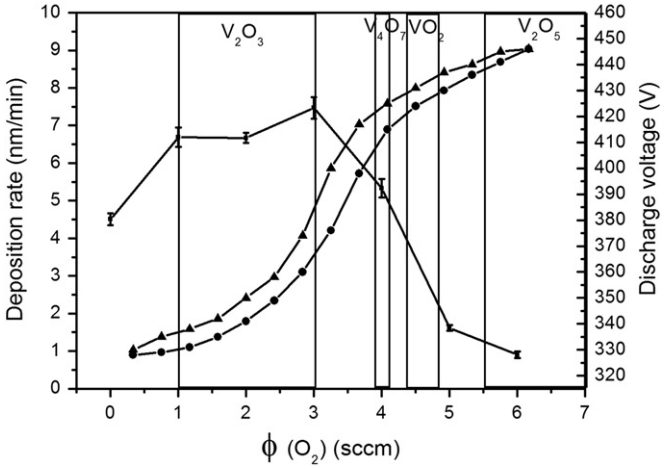


**Fig. 1.** Deposition rate (■) and discharge voltage (go ●–return ▲) as a function of the oxygen flow rate (ϕ).

With increasing oxygen flux, a decrease of the deposition rate was observed due to target poisoning as indicated by the discharge voltage behaviour. Different oxide stoechiometries were observed depending on the oxygen flux. From systematic X-Ray Diffraction (XRD) measurements on several sets of samples prepared with different $O_2$ flux values, four structural ranges were identified going from $V_2O_3$ to $V_2O_5$. As shown in Fig. 2, $V_2O_3$ films could be obtained with $O_2$ fluxes ranging from 1 to 3 sccm. At 4 sccm, $V_4O_7$ film was formed and at 4.5 sccm single polycrystalline $VO_2$ phase was prepared. At 5 sccm, an amorphous film was deposited while for higher fluxes, multiphase films were formed with a high concentration of $V_2O_5$. As expected, $VO_2$ thin films were obtained in a very narrow range in the metal-oxide transition domain. Using a DC discharge power density of 9.87 W/cm$^2$, the growing rate was 3.5 nm/min.

### 4.2. Optical properties

The ellipsometric spectra of the metallic substrate were recorded in the 0.3 to 17.5 μm spectral range for three different angles of incidence (65°, 70° and 75°) and the optical properties were extracted using the pseudo-dielectric function ⟨ϵ⟩:

$$\langle\epsilon\rangle \; sin^2\phi + \; sin^2\phi \; tan^2\phi \frac{(1-\rho)^2}{(1+\rho)^2}$$

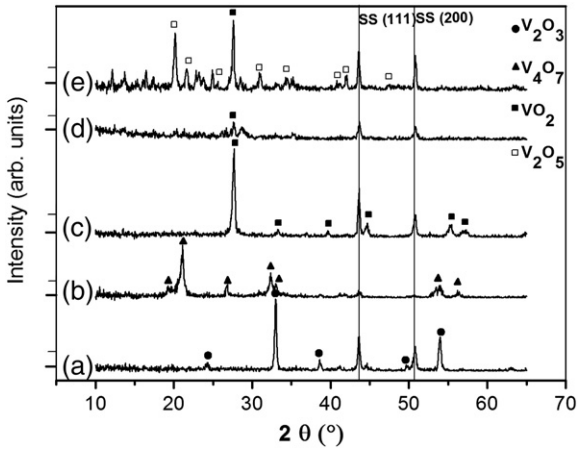


**Fig. 2.** Grazing incidence (1°) XRD patterns of $VO_x$ films deposited at different oxygen flux : (a) 3 sccm (b) 4 sccm (c) 4.5 sccm (d) 5 sccm (e) 7 sccm.

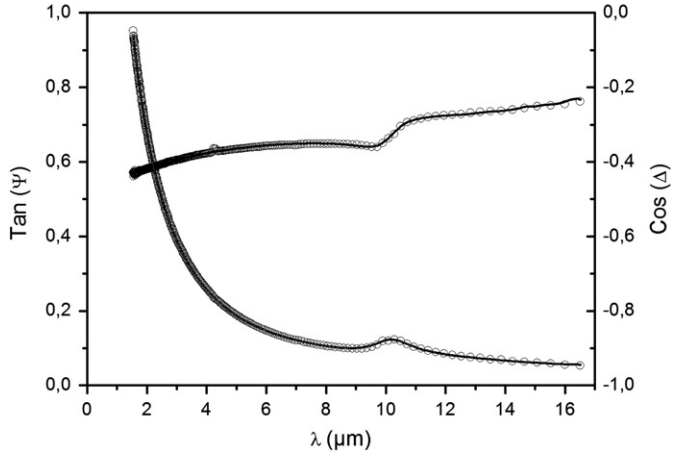


**Fig. 3.** Ellipsometric spectra of the 200 nm-thick sample in the infrared at 100 °C—open circles : experimental data—plain lines : simulated data.

where $\rho = \tan\psi e^{i\Delta}$ is the ellipticity, $\psi$ and $\Delta$ the ellipsometric angles and $\phi$ the angle of incidence. Results showed that the pseudo-indices did not depend on the incidence angle $\phi$, confirming the 'bulk' nature of the substrate. Similar experiments were run on annealed substrates (20 min at 480 °C) in order to estimate the influence of the annealing of the metal during the deposition process. In that case, the pseudo-indices approach did not appear to be valid anymore and the so-calculated indices depend on the incidence angle in the infrared spectral range ($\lambda > 2.8$ μm). To circumvent this drawback, a thin dielectric layer (thickness: $d_r = 12$ nm, dielectric constant: $\varepsilon_r = 16.2$) has been introduced in the optical stack modelling.

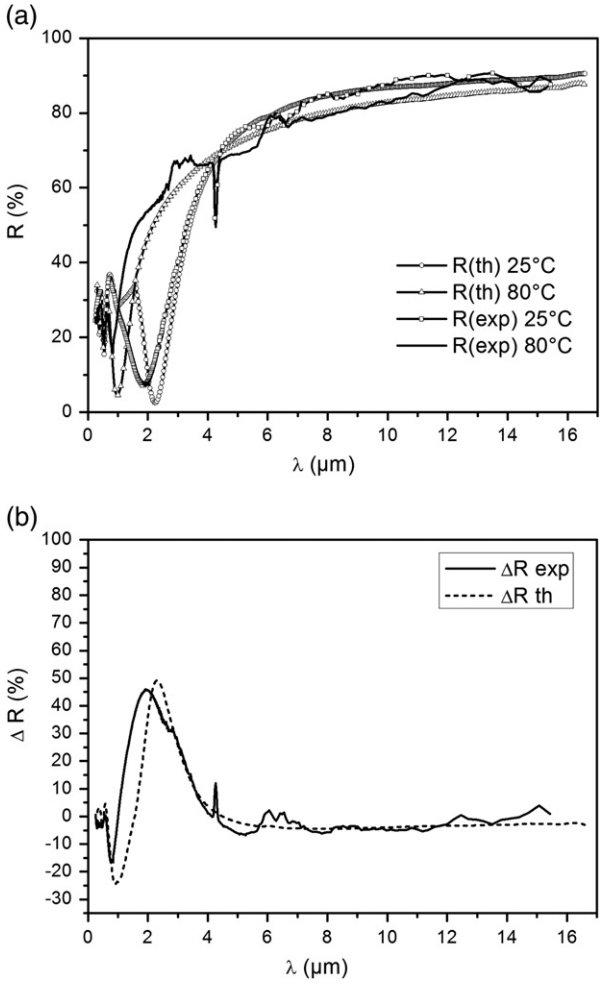


**Fig. 4.** (a) Experimental (Rexp) and theoretical (Rth) spectral reflectance of 100 nm thick $VO_2$ film on stainless steel at room temperature and at 80 °C. (b) Contrast spectra of 100 nm thick $VO_2$ film on stainless steel.

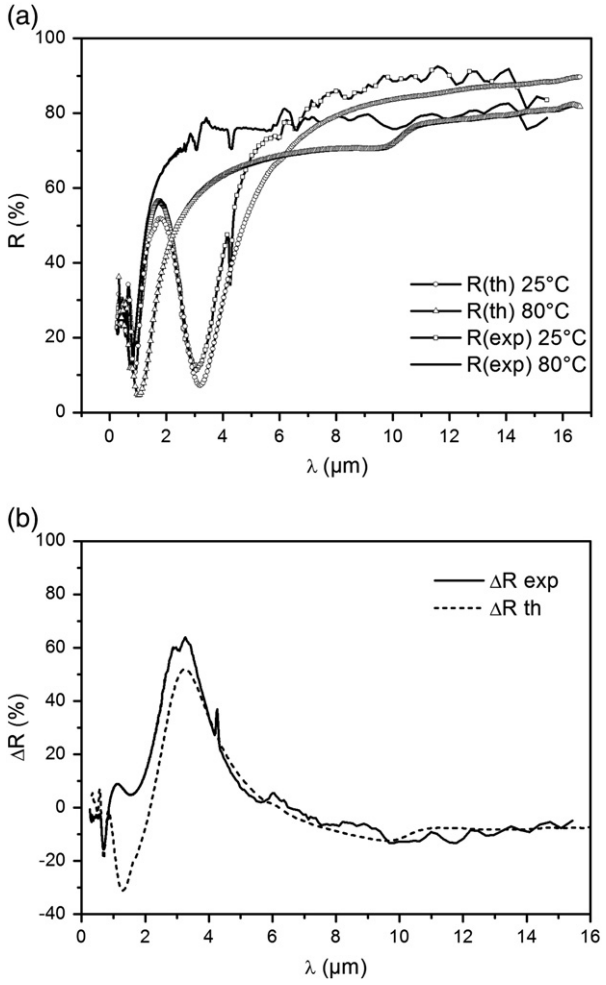


**Fig. 5.** (a) Experimental (Rexp) and theoretical (Rth) spectral reflectance of 200 nm thick $VO_2$ film on stainless steel at room temperature and at 80 °C. (b) Contrast spectra of 200 nm thick $VO_2$ film on stainless steel.

The optical constants and thicknesses of the $VO_2$ layers were determined by fitting simultaneously the thickness of the layer and

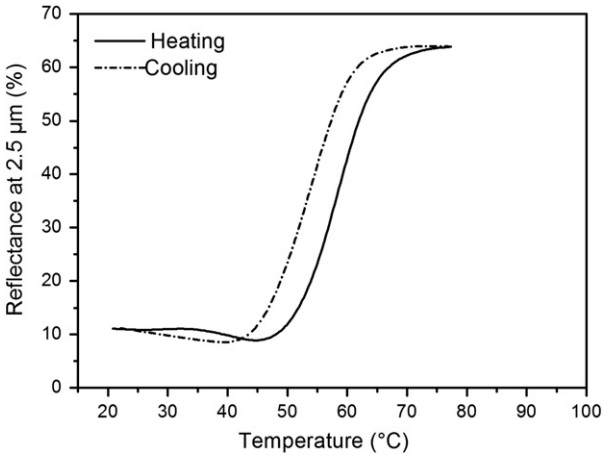


**Fig. 6.** Optical switching in reflectance at 2.5 μm of 200 nm film of $VO_2$ on stainless steel.

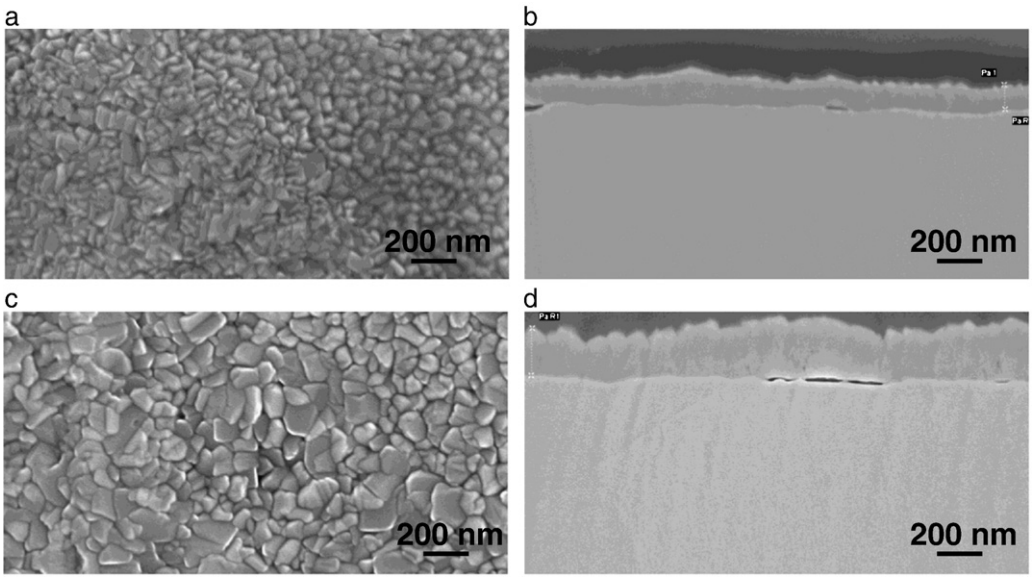


**Fig. 7.** SEM micrographs of $VO_2$ thin films with different thicknesses : (a) 100 nm film top view (b) 100 nm film cross section (c) 200 nm film top view and (d) 200 nm film cross section.

the parameters of a Cauchy-type dispersion law for the real and imaginary parts of the complex refraction index, *n* and *k* respectively. Absorption peaks in the *k* spectrum were modelled as non-interacting Lorentzian peaks and, at 100 °C, an additional Drude contribution was considered to account for the transition between the semiconductor state and the metallic one. Fig. 3 shows the ellipsometric experimental and simulated data in the infrared at 100 °C. Due to the possible thickness inhomogeneity of the layers and of the possible subsequent depolarisation, a roughness layer was included in the optical model using a Bruggeman effective media approximation [13]. The simulated ellipsometric spectra are in good agreement with the experimental ones.

Reflectance spectra of 100 nm and 200 nm thick $VO_2$ films were measured from $\lambda = 0.25$ to 15 μm, both at room temperature and at 80 °C. On the theoretical side, we used the measured refractive index in order to calculate the reflectance spectra. These calculations were performed for both temperatures as well. The reflectance spectra at high and low temperatures ($R_{HT}$ and $R_{LT}$ respectively) and the contrast spectrum ($\Delta R = R_{HT} - R_{LT}$) are displayed in Fig. 4 for the 100-nm thick film and in Fig. 5 for the 200-nm thick film. It is important to note that for these simulations, we used the experimental thickness values that were obtained from profilometry measurements on the samples. The good agreement between experimental and theoretical spectra justifies our method (of course, curve fitting could be further improved by tuning slightly the thickness values). Our measurements cover the complete UV-VIS–IR range and therefore show the reliability of our model in performing simulations with measured refractive indices. The reflectance spectra at room temperature exhibit a local minimum around 2.5 μm where the optical contrast is around 55%. Then, even if the $VO_2$ is in its transparent state, the reflectance increases very much due to the contribution of the metallic substrate. At 80 °C, the reflectance of the $VO_2$-coated substrate in the infrared region is around 80–90%.

The monitoring of the infrared reflectance at $\lambda = 2.5$ μm as a function of temperature showed a hysteresis curve (Fig. 6). The transition temperature ($T_C$) was found to be around 64 °C in our samples. This value is lower than the $T_C$ observed for $VO_2$ single crystal or thin films reported by other authors [2,14–17]. This low $T_C$ could be due to the thermal stress induced in the film during the growth of the film and during its subsequent cooling step (22 °C/min) applied after deposition. This thermal stress could result from the high difference between thermal expansion coefficients of the film and the substrate, as demonstrated previously [18,19]. The width of the hysteresis loop (full width at half maximum) is narrow (5 °C) indicating that the film is made of large grains [15].

The morphologies of the $VO_2$ films are shown in Fig. 7. For a film thickness of 100 nm, the structure appears to be made of small well-defined grains with an average size of about 50 nm, which become larger (150 nm) for 200 nm film thickness. On the cross section, columnar structure and adhesion failure can be observed. The internal thermal stress could be also responsible for a lack of adherence.

## 5. Conclusions

Thin thermochromic films of vanadium dioxide were deposited on stainless steel with an accurate control of the oxygen flux. The reflectance spectra of the $VO_2$-coated steel material were predicted using a theoretical model based on a continued-fraction calculation method which was developed for arbitrarily stratified media. Theoretical predictions were found to be in good agreement with the experimental measurements, which shows the validity of the modelling approach. The existence field of $VO_2$ is quite narrow, so a complementary study to optimise the deposition process of thermochromic films on stainless should be led.

## Acknowledgments

This work is partially funded by the Ministère de la Région Wallonne, the European Community and the Fonds National de la Recherche Scientifique (FNRS) of Belgium. S. G.-S and H.K are supported by Mirage project under reference : MIRAGE-RRW-TECPART-LPS with convention 5579. M.V. thanks J.L. Stehlé, J.P Piel and C. Defranoux (Sopralab) for the support in the ellipsometric measurements analysis.

## References

[1] P. Jin, G. Xu, M. Tazawa, K. Yoshimura, Appl. Phys. A 77 (2003) 455.
[2] P. Jin, S. Tanemura, Jpn. J. Appl. Phys. 33 (1994) 1478.
[3] P. Jin, T. Miki, K. Yoshimura, M. Tazawa, Y. Tai, S. Tanemura, Front. Sci. Ser. 7 (1993) 301.
[4] G. Xu, P. Jin, M. Tazawa, K. Yoshimura, Sol. Energy Mater. Sol. Cells 83 (2004) 29.
[5] K.A. Khan, G.A. Niklasson, C.G. Granqvist, J. Appl. Phys. 64 (1988) 3327.
[6] K.A. Khan, C.G. Granqvist, Appl. Phys. Lett. 55 (1989) 4.
[7] C.H. Griffiths, H.K. Eastwood, J. Appl. Phys. 45 (1974) 2201.
[8] G. Xu, P. Jin, M. Tazawa, K. Yoshimura, Jpn. J. Appl. Phys. 43 (2004) 186.

[9] K.L. Lewis, A.M. Pitt, T. Wyatt-Davies, J.R. Milward, Mater. Res. Soc. Symp. Proc. 374 (1995) 105.
[10] R.T. Kivaisi, M. Samiji, Sol. Energy Mater. Sol. Cells 57 (1999) 141.
[11] M. Tazawa, P. Jin, S. Tanemura, Appl. Opt. 37 (1998) 1858.
[12] A. Dereux, J.P. Vigneron, P. Lambin, A.A. Lucas, Phys. Rev. B 38 (1988) 5438.
[13] D.E. Aspnes, J.B. Theeten, F. Hottier, Phys. Rev. B 20 (1979) 3292.
[14] F. Guinneton, L. Sauques, J.-C. Valmalette, F. Cros, J.-R. Gavarri, Thin Solid Films 446 (2004) 287.
[15] D. Brassard, S. Fourmaux, M. Jean-Jacques, J.-C. Kieffer, M.A. El Khakani, Appl. Phys. Lett. 87 (2005) 051910.
[16] E. Chain, Appl. Opt. 30 (1991) 2782.
[17] M. Soltani, M. Chaker, E. Haddad, R.V. Kruzelecky, D. Nikanpour, J. Vac. Sci. Technol., A 22 (2004) 859.
[18] Y. Ningyi, L. Jinhua, H.L.W. Chan, L. Chenglu, Appl. Phys. A: Mater. Sci. Process. 78 (2003) 777.
[19] F. Beteille, L. Mazerolles, J. Livage, Mater. Res. Bull. 34 (1999) 2177.